

# STABILIZATION OF THE POLARIZATION PLANE IN TRAVELLING WAVE DEFLECTORS

N.Sobenin, M.Lalayan, S.Kutsaev, A.Anisimov A.Smirnov, I.Isaev,  
 Moscow Engineering-Physics Institute, Moscow, Russia

A.Zavadtsev, D.Zavadtsev,  
 «Nano Invest», Moscow, Russia

## Abstract

New possibilities of the polarization plane stabilization in the traveling hybrid  $TM_{11}$  wave deflectors are considered in this paper. These possibilities are realized in two new structures: DLW with two peripheral recesses in cells and DLW with oval aperture. In terms of electrodynamic parameters, thermal regimes and manufacturing technology these structures as well as a classical structure with two stabilizing holes show some advantages and some disadvantages. The advantages of the new structures are good RF mode separation and effective cooling. The specifics of such structures tuning are also described.

## INTRODUCTION

Nowadays linear electron beams accelerated in the superconducting accelerating structures are often used in free electron lasers as core elements. The brightness of the coherent radiation could be very high in case of high average power of the electron beam. Wide variation of wave length is achievable down to X-ray band. The accelerated beam quality is a concern for advanced free electron lasers and therefore these facilities must be equipped with dedicated beam control and measuring system. The deflecting system deviates selected bunches from train and directs them to bunch length monitor and phase space analyzing equipment. Traveling wave RF deflector with transverse electric field  $E_d$  is used for this purpose. Disk loaded waveguide (DLW) operating on hybrid  $TM_{11}$  mode is a good choice for deflector. The field polarization plane is often set by two holes made oppositely in the diaphragm [1,2]. Along with this conventional design new solutions namely DLW with oval beam aperture and DLW with two peripheral recesses at cell equator were considered. The traveling wave RF deflector with the phase advance  $\theta = 120^\circ = 2\pi/3$  and with relative phase velocity  $\beta_{ph} = v_{ph}/c = 1$  is the most practical choice to combine electrodynamic performance and reasonable production procedure.

## ELECTRODYNAMICAL CHARACTERISTICS OF THE DEFLECTING STRUCTURE

The deflecting voltage  $V_\perp$  in the constant impedance DLW with the same shape of all cells in the structure is determined by following formula:

$$V_\perp = \int_0^l E_{0\perp} e^{-\alpha z} dz = \frac{E_{0\perp}(1 - e^{-\alpha l})}{\alpha}$$

$$\frac{E_{0\perp} \lambda}{\sqrt{P}} = \sqrt{\frac{2\pi \lambda r_{sh\perp}}{\beta_g Q}}$$

$$r_{sh\perp} = \frac{\left( \int_0^l |E_z(z)_{x=a}| dz \right)^2}{(ka)^2} \frac{1}{Pl} = \frac{V_\perp^2}{Pl}$$

where  $P$  is the input RF power,  $\alpha = \pi f / (c\beta_g Q)$  is wave attenuation factor,  $l$  is the length of the structure,  $\beta_g$  is relative group velocity,  $Q$  is Q-factor,  $\lambda$  is the operating wavelength,  $r_{sh\perp}$  is transverse shunt impedance,  $a \sim 1\text{mm} < R_a$  is the small distance from the axis in deflecting plane,  $k = 2\pi/\lambda$ . The higher  $\beta_g$  value leads to higher value of input power  $P$  to provide required deflecting field  $E_d$ .

To satisfy the requirements for filling time and deflecting voltage, the structure should have normalized deflecting field (frequency independent parameter of the structure):

$$\frac{E_{0\perp} \lambda}{\sqrt{P}} \approx 220 \text{ Ohm}^{1/2}, |\beta_g| > 0.015$$

To have tolerable short-range wakefield parameters for the structure, the aperture radius must be  $R_a > 20$  mm.

Parameters of RF deflector should be defined as a compromise between discrepant requirements of shorter filling time and tolerable input RF power. To provide short filling time

$$\tau = \frac{l}{c\beta_g}$$

we are interested to have higher group velocity

The hybrid  $TM_{11}$  wave in the DLW is twice degenerated, introducing mode mixing problem and deflecting plane instability. The orientation of the deflecting plane must be stabilized. The possible deviation should be not more than  $0.5^\circ$ . To stabilize deflecting plane orientation, the dispersion curve of the waves with perpendicular field orientation must be shifted in frequency with respect to the dispersion curve of the deflecting wave. The possible deviation of deflecting field orientation due to mode mixing is inverse proportional to the frequency separation between dispersion curves.

## CONSIDERED DEFLECTING STRUCTURES

Several DLW based structures, shown in Fig 1, were considered for RF deflector: the structure with two stabilizing holes, Fig.1a, (well known LOLA structure [1]), the structure with oval aperture (Fig.1b, Fig. c) and the structure with two peripheral recesses (Fig.1d). Similar to LOLA structure all structures are backward wave operating with phase advance  $\theta=120^\circ$ , except structure with bigger oval aperture (Fig.1c) operating on forward wave. The RF parameters of these structures for operating frequency  $f=3$  GHz are summarized in the Table 1. All structures have the same iris thickness  $t_d=5.4$  mm and iris tip rounding radius  $R_c=t_d/2$ .

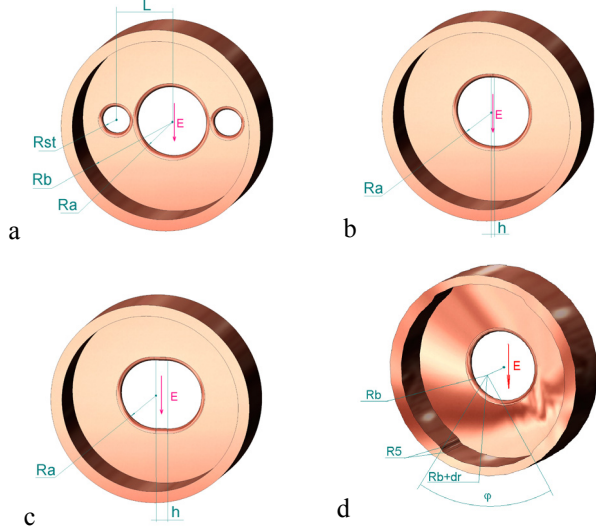


Figure 1: DLW based deflecting structures: with two stabilizing holes (a), with smaller (b) and bigger (c) oval aperture and with two peripheral recesses (d). The deflecting plane orientation is vertical.

Table 1: Dimensions and RF parameters of the structures. Operating frequency  $f_0=f_{\text{def}2\pi/3}=3$  GHz,  $\Theta=120^\circ$ ,  $\Delta f_1=|f_0-f_{\text{per}2\pi/3}|$ ,  $\Delta f_2=|f_0-f_{\text{def}\pi}|$ ,  $\Delta f_3=|f_0-f_{\text{per}\pi}|$

Parameter	Structure			
	Fig.1a	Fig.1b	Fig.1c	Fig.1d
$L$ , mm	34.65	-	-	-
$R_{st}$ , mm	9.0	-	-	-
$h$ , mm	-	1.7	6.5	-
$\varphi$ , град	-	-	-	65
$dr$ , mm	-	-	-	1
$R_a$ , mm	21.55	20.5	21.5	21.5
$R_b$ , mm	55.27	55.49	53.45	55.03
$\alpha$ , 1/m	0.153	0.125	0.121	0.144
$\beta_g$	-0.017	-0.020	0.020	-0.018
$r_{sh\perp}$ , MOhm/m	17.15	19.34	17.71	17.21
$Q$	11840	12360	12530	12400

$\Delta f_1$ , MHz	-30	-30	-147	-28
$\Delta f_2$ , MHz	-11	13	-16	11
$\Delta f_3$ , MHz	-24	-17	-157	-18
$E_{0\perp}\lambda/\sqrt{P}$	229	220	221	223
Ohm <sup>1/2</sup>				

The structure with two peripheral recesses has essential reserve in the mode separation and obtained result is not a limit. The cell dimensions of the structure with bigger oval aperture (Fig. 1c) are chosen to have both the positive dispersion and much bigger frequency separation with significantly deformed dispersion curve of the perpendicular polarization.

The calculated sensitivity of the structure frequency to the main manufacture tolerances is shown in Table 2. These data are obtained for the structure presented in Fig.1d.

Table 2: Sensitivity of the structure frequency to the main manufacture tolerances (MHz/mm)

$\frac{df}{dR_b}$	$\frac{df}{dR_a}$	$\frac{df}{dt}$	$\frac{df}{dR_c}$	$\frac{df}{d(dr)}$
-48.5	-16.3	4.0	-3.9	-28

## MAXIMAL ELECTRIC AND MAGNETIC FIELDS AT THE STRUCTURE SURFACE

The maximal values of electric  $E_{sm}$  and magnetic  $H_{sm}$  fields on the TDS surface during operation are determined by the value of deflecting field value  $E_d$

$$E_d = 1/(kal) \int_0^l E_{z(r=a)} e^{-ikz} dz, \quad k = (2\pi f)/c$$

In the DLW based structure with hybrid TM11 wave maximal values of electric and magnetic field are essentially localized at the iris tip. Max  $E_{sm}$  value is at the iris in the deflecting plane and max  $H_{sm}$  value is at the iris in the perpendicular plane along specified curve. These fields distribution on the structure surface have been calculated. These values were extrapolated using several values at different elevations over the surface in order to omit mesh effects.

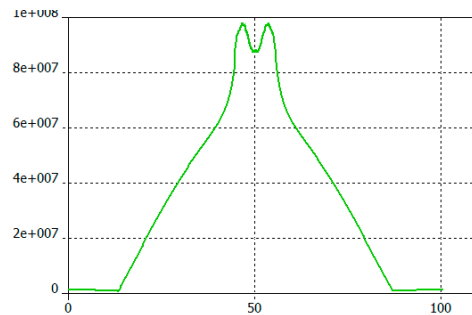


Figure 2: Electric field (relative values) distribution along the generating line (mm) of the cell diaphragm.

The values of  $E_{sm}/E_d$  and  $E_{sm}/H_{sm}$  were calculated along the generating line of the cell diaphragm. For the cells dimensions mentioned above the values are  $E_{sm}/E_d = 4.35$  and  $E_{sm}/H_{sm} = 272$  Ohm.

### INPUT & OUTPUT COUPLER

The coupler model is shown in Figure 3. The coupling factor of the waveguide with the structure is determined by the width  $X$  of the coupling window ( $X=32.45$  mm in Figure 3). The eigen frequency of the coupler cell is determined both by the width  $X$  of the coupling window and by the cell radius  $R_b$  ( $R_b = 53.73$  mm in Figure 3). Both input and output couplers of the model were tuned simultaneously. The reflection  $S_{11}$  inside the structure was calculated. The transverse electric field in the iris cross section was used to determine the reflection  $S_{11}$  inside the structure. Minimum of the function  $S_{11}$  inside the structure of two variables  $X$  and  $R_b$  has been found. These values of  $X$  and  $R_b$  correspond to the tuned coupler. Frequency responses to radius and coupling window width equal to  $\partial f/\partial R_b = 13,1$  MHz/mm and  $\partial f/\partial X = -3,8$  MHz/mm.

Reflection  $S_{11}$  in input waveguide port of the 16-cell structure is shown in Fig.4.

Cut-off waveguides provide attenuation as high as  $-42$  dB/100 mm.

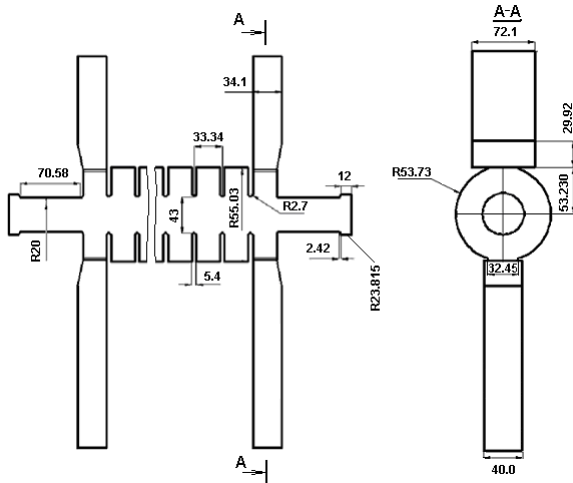


Figure 3: The simulation model of the structure with two couplers with auxiliary cut-off waveguides.

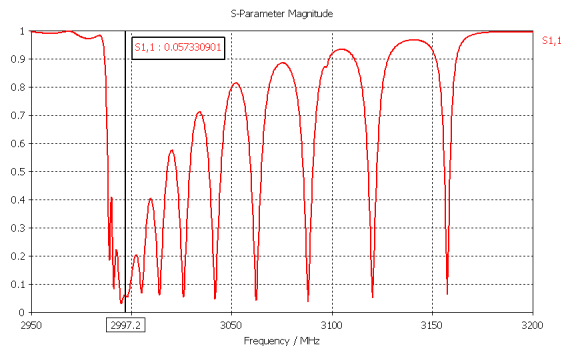


Figure 4: Reflection  $S_{11}$  in the input waveguide port of the 16-cell structure. Operating mode frequency is 2997.2 MHz.

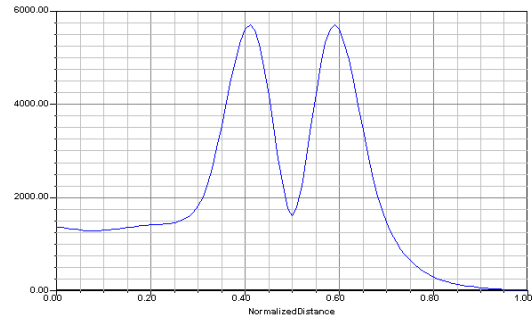


Figure 5: Electric field complex amplitude distribution along rectangular waveguide axis, coupler and cut-off waveguide axis (structure axis corresponds to the distance equaled to 0.50).

### THERMAL STRESS ANALYSIS

Thermal simulations were made for all considered copper-made structures with water cooling channels. Different cooling system layouts were compared: two or four of cooling rectangular pipes (16x7.9 mm). The calculated temperature map in the cavity cell (Table 1, Fig.1d) at the 26 MW input power for the structure equipped with two and four cooling pipes are presented in Fig.6.

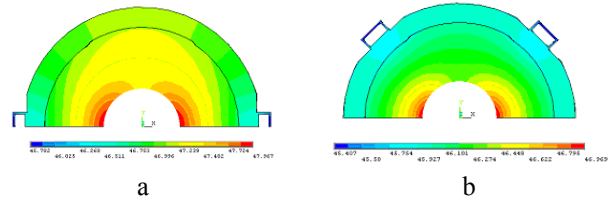


Figure 6: Temperature map ( $^{\circ}\text{C}$ ) in the cell at 26 MW input power for two (a) and four (b) cooling channels.

### CONCLUSIONS

The new deflecting DLW structures (Fig.1 b, c and d) have low surface electric field strength and 1.2 times lower temperature gradient. The manufacture of these structure cells is possible using program-controlled machine, but the manufacture of the structure with two recesses is simpler. According to all data the shape with two recesses at cavity equator presented on Fig.1d is the most preferable for deflector.

### ACKNOWLEDGEMENTS

Authors would like to thank L. Kravchuk, V. Paramonov, M. Huening and F. Stephan for helpful discussions.

### REFERENCES

- [1] Akle R. et al., A Transverse RF Deflecting Structure for Bunch Length and Phase Space Diagnostics, SLAC-PUB-8864, June 2001, 36p.
- [2] Sobenin N.P., Zverev B.V., Electrodynamics Characteristics of Accelerating Cavities, Foundation for International Scientific and Education Cooperation, London, England, 1999, 288p.